Biomaterials 97 (2016) 154–163

Contents lists available at ScienceDirect

Biomaterials

journal homepage: www.elsevier.com/locate/biomaterials

A versatile plasmonic thermogel for disinfection of antimicrobial resistant bacteria

Mohamed A. Abdou Mohamed [a, b, f, 1], Vahid Raeesi [b, e, 1], Patricia V. Turner [j], Anu Rebbapragada [h], Kate Banks [g, i], Warren C.W. Chan [a, b, c, d, e, *]

[a] Institute of Biomaterials and Biomedical Engineering, University of Toronto, 164 College St. 407, Toronto, ON, Canada
[b] Donnelly Centre for Cellular and Biomolecular Research, University of Toronto, 164 College St. 407, Toronto, ON, Canada
[c] Chemistry, University of Toronto, 164 College St. 407, Toronto, ON, Canada
[d] Chemical Engineering, University of Toronto, 164 College St. 407, Toronto, ON, Canada
[e] Materials Science and Engineering, University of Toronto, 164 College St. 407, Toronto, ON, Canada
[f] Botany and Microbiology Department, Faculty of Science, Zagzig University, Zagazig, Egypt
[g] Division of Comparative Medicine, Faculty of Medicine, University of Toronto, Toronto, ON, Canada
[h] Gamma-Dynacare Medical Laboratories, Brampton, ON, Canada
[i] Department of Physiology, Faculty of Medicine, University of Toronto, Toronto, ON, Canada
[j] Department of Pathobiology, University of Guelph, Guelph, ON, Canada

ARTICLE INFO

Article history:
Received 26 January 2016
Received in revised form
11 April 2016
Accepted 18 April 2016
Available online 22 April 2016

Keywords:
Photothermal
Gold nanorods
Thermogel
Wound infections
Antibiotic resistant bacteria

ABSTRACT

The increasing occurrence of antimicrobial resistance among bacteria is a global problem that requires the development of alternative techniques to eradicate these superbugs. Herein, we used a combination of thermosensitive biocompatible polymer and gold nanorods to specifically deliver, preserve and confine heat to the area of interest. Our data demonstrates that this technique can be used to kill both Gram positive and Gram negative antimicrobial resistant bacteria in vitro. Our approach significantly reduces the antimicrobial resistant bacteria load in experimentally infected wounds by 98% without harming the surrounding tissues. More importantly, this polymer-nanocomposite can be prepared easily and applied to the wounds, can generate heat using a hand-held laser device, is safe for the operator, and does not have any adverse effects on the wound tissue and healing process.

1. Introduction

Antimicrobial resistance (AMR) is a global problem that represents a major threat to human and animal health. Multidrug resistant superbugs are often hospital or community acquired sources of infection of the lungs, urinary tract, gastrointestinal tract, skin and soft tissue. It is estimated that AMR causes 2 million illnesses and 23 thousand deaths annually in the United States [1]. The clinical management of skin and soft tissue infections alone represents an increasing economic burden, estimated to surpass $4.8 billion/year in health care costs in the United States [2]. Complications associated with these infections are common, occurring in up to 25% of cases, and include bacteremia, endocarditis, and sepsis [3]. Taken together, there is an urgent need to develop effective alternative antimicrobial therapies for AMR infections.

At the correct temperature, heat can be used to destroy bacteria through disruption of the cell membrane, fatty acid melting, and protein denaturation [4]. However, one challenge in using heat to treat wounds is to locally and selectively concentrate and deliver the heat to the infected area without damaging the surrounding tissue. Inorganic nanoparticles (NP) offer fine control and homogenous distribution of heat over conventional heating probes, such as ultrasound, microwaves, and radiofrequency [5]. There are several types of heat-producing NPs including gold nanomaterials, magnetic NPs, carbon-based nanostructures, and porphysomes [6–9]. Typically, these particles are excited by light or magnetic fields and the resulting energy is converted into heat through atomic scale electronic and orientation transitions [10]. When NPs

* Corresponding author. Institute of Biomaterials and Biomedical Engineering, University of Toronto, 164 College St. 407, Toronto, ON, Canada.
E-mail address: warren.chan@utoronto.ca (W.C.W. Chan).
[1] These authors contributed equally.

http://dx.doi.org/10.1016/j.biomaterials.2016.04.009
0142-9612/

are excited by light, the process is known as photothermal therapy (PTT). The predominant applications of PTT have been: 1) localized ablation of diseased tissues; 2) as diagnostic probes; and 3) to manipulate and control the release of drugs [6,11,12]. Previous studies have demonstrated that PTT can be used to selectively kill AMR bacteria in vitro [13–16]. However, to apply this technique to the treatment of infected wounds in-vivo, an appropriate NP dispersion medium is required. Since the NP dispersion medium used to perform PTT experiments is water, a major limitation is evaporation, resulting in poor heat delivery and preservation.

In this study, we devised a PTT technique to specifically deliver, preserve, and confine heat to a defined area. We used a combination of a thermosensitive biocompatible polymer, n-vinyl-polycaprolactam (PVCL), as a dispersion medium, and gold nanorods (NRs) excited by a low intensity laser. PVCL is a biocompatible polymer that exhibits phase transition from sol to gel upon heating. Once in gel form this polymer can confine and preserve heat generated from NPs dispersed within it to a defined area of interest. NRs were selected because of ease of synthesis and functionality, as they possess high absorption cross-section and are able to absorb light at between 700 and 1000 nm (a region of the electromagnetic spectrum with low biological scattering and absorption). We hypothesized that this PTT method could have potent bactericidal effect when applied to experimentally infected wounds created using a standard biopsy punch in rats.

2. Materials and methods

2.1. Gold nanorods synthesis, functionalization and characterization

Gold nanorods were synthesized using a seed-mediated method described by Nikoobakht and El-Sayed and Gou and Murphy [17,18] with modifications. Briefly, the seed solution was prepared by adding 1.2 ml of 0.01 M sodium borohydride (Sigma-Aldrich, St. Louis, MO, USA) to 20 ml scintillation vial that contains 500 μL of 0.01 M gold chloride (Sigma-Aldrich, St. Louis, MO, USA) and 19.5 ml 0.1 M cetyl trimethylamonnium bromide (CTAB) (Sigma-Aldrich, St. Louis, MO, USA) under vigorous stirring. In a clean bottle, 49.5 ml of 0.01 M gold chloride was added to 950 ml of 0.1 M CTAB. To that, 5 ml of 0.01 M $AgNO_3$ (Sigma-Aldrich, St. Louis, MO, USA) and 7 ml of 0.1 M ascorbic acid (Sigma-Aldrich, St. Louis, MO, USA) were added respectively under stirring. Finally, 20 ml of the above prepared seed solution was added and the entire solution was left overnight with constant stirring. The obtained gold nanorod solution was then purified by centrifugation twice at 17000 g for 20 min and re-dispersed in deionized water to remove excess CTAB. The CTAB-NRs were further characterized using UV–Vis spectrophotometer (Shimadzu, UV-1601PC) and zeta potential. For surface functionalization, 5 ml of the above concentrated CTAB-NRs solution was added to clean bottle containing a solution of m-PEG-SH (MW: 5000 Daltons, Laysan Bio) so that the final concentration of PEG was 0.5 mg/ml. The mixture was incubated at room temperature for 4 h. PEG coated NRs (PEG-NRs) were further purified twice by centrifugation at 17000 g for 20 min to remove excess PEG and CTAB. PEG-NRs were further characterized using UV–Vis spectrophotometer, zeta potential (Nano-Zs) and Transmission Electron microscopy (TEM) (Hitachi 7000).

2.2. Preparation and characterization of gold nanorods thermogel nanosol

21.5% w/v of Poly N-vinylcaprolactam (PVCL) (MW: ~176000 Daltons, PolySciTech Akina, Inc) solution prepared by dissolving equivalent amount of polymer in 1x phosphate buffered saline buffer (PBS) (2.7 mM potassium chloride, 173 mM sodium chloride and 1.76 mM potassium phosphate) at 4 °C overnight. This was followed by addition of the above prepared PEG-NRs to the polymer solution so that the final concentration of NRs and polymer was 5 nM and 20%, respectively. The thermogel nanosol solution was further characterized by UV–Vis spectrophotometric measurement and TEM.

2.3. Development of temperature profiles

The rise in temperature of 3 different solutions of the NRs was measured using an infrared (IR)-Camera (ICI 7320) for 20 min. First, 1.5 μL of 400 nM PEG-NRs were dispersed in 56.5 μL of 21.5% w/v PVCL, 1xPBS and 21.5% w/v PEG solutions respectively. 2 μL of 1xPBS was then added to all solutions so that the final volume was 60 μL. Then 50 μL of each solution was applied on the surface of 35 mm Petri dish followed by laser irradiation using 785 nm continuous wave diode laser as light source (0.65 W/cm^2) for 20 min. The rise in temperature (ΔT_f) was calculated as the difference between film temperature at time point t (Tf(t)) and initial film temperature (T_0 ~ 18.5 ± 1.5) on the surface. Blank solutions of PVCL, PBS and PEG were used as non-heating controls.

2.4. Heat dissipation and water evaporation measurements

1.5 μL of 400 nM PEG-NRs was dispersed in 56.5 μL of 21.5% w/v PVCL and 1xPBS. 2 μL of 1xPBS was then added to all solutions so that the final volume was 60 μL. Then 50 μL of each solution was applied on the surface of 35 mm Petri dish followed by laser irradiation at 0.65 W/cm^2 for NRs-PVCL and 1.5 W/cm^2 for NRs-PBS. After 10 min of exposure, the laser was turned off and the drop of temperature from the two solutions was measured as described above. For water evaporation measurement, 50 μL of each solution was weighed before and after laser exposure using analytical scale (METTLER TOLEDO, AL54, readability 0.0010), and the amount of evaporated water was calculated as:

$$\%\ of\ water\ evaporation = (W_b - W_a/W_b) \times 100$$

where W_b is the weight (g) of sample before laser exposure and W_a is the weight (g) of sample after laser exposure.

2.5. Antimicrobial effect of gold nanorods thermogel in vitro

Three antibiotic resistant bacteria have been used in this study. Ampicillin-resistant *Escherichia coli* NEB 10 beta was obtained from Dr. Aaron Wheeler's lab (Chemistry Department, University of Toronto, Canada). Vancomycin, ampicillin, and gentamicin-resistant *Acinetobacter baumannii* and vancomycin resistance *Enterococcus faecalis* (VRE) ATCC51299 were obtained from Dr. Justin Nodwell's lab (Biochemistry Department, University of Toronto, Canada). Overnight cultures of *E. coli*, *A. baumannii* and *E. faecalis* bacteria were prepared by streaking small amount of the frozen bacterial stock on Luria agar (LA) plates and incubated at 37 °C. Then a single colony of each bacteria was inoculated in Luria broth (LB) medium and incubated at 37 °C while shaken (200 rpm). Fresh cultures were prepared in LB medium by adding 30 μL of overnight culture to 2.97 ml of LB media and incubating for another 3–4 h at 37 °C while shaken or until the OD_{600} of the culture medium reached approximately 0.3–0.4 (logarithmic growth phase). The bacteria pellets were then collected by centrifugation at 3000 *g* for 10 min and then washed three times with sterile PBS. The pellets were then re-suspended in an appropriate amount of sterile PBS buffer for further use. To test the antimicrobial effect of NRs-PVCL, 2 μL of bacterial cultures was

added into 56.5 μL of 21.5% PVCL followed by addition of 1.5 μL of 400 nM PEG-NRs. The samples were then exposed to laser (0.65 W/cm^2) for 10, 20 and 40 min and up to 60 min for *E. faecalis*. The percentage of living cells was calculated by dividing colony forming unit CFU/ml of sample by CFU/ml of control (bacteria in PBS without any treatment). Briefly, 450 μL of PBS was added to the sample in the 35 mm Petri dish and then transferred to centrifuge tubes for further dilutions. 100 μL of each dilution was inoculated on LA plates. After 24 h of incubation at 37 °C, colonies on the plates were counted and % of living cells was calculated as mentioned earlier. All the control experiments that have been done to test the antimicrobial effect of NRs-PBS + Laser, laser without NRs and NRs without laser were conducted similarly.

2.6. TEM for in vitro study

NRs-PVCL photothermal treated and non-treated bacterial cells were pelleted and washed thrice in PBS by centrifugation. Residual PBS was decanted. Cells were fixed in electron microscopy fixative for 1 h at room temperature, stained, and sliced onto a TEM grid for visualization using TEM (FEI Tecnai 20).

2.7. Surgical wound creation

Rats were anesthetized using isoflurane (5% induction, 2–3% maintenance) in 100% oxygen. Ketoprofen was administered as analgesic (5 mg/kg, SC, once daily for 2 d). For surgical preparation, the rat dorsum was shaved and a hair removing cream (Nair, Church and Dwight Canada Corp, Canada) was applied to ensure complete hair removal. The skin was disinfected by two successive swabs of 70% ethanol followed by betadine (Rougier Pharma, Canada) and a sterile drape was placed over the rat. A sterile 5 mm biopsy punch (Miltex Inc, USA) was used to make 2 circular full thickness wounds centered just cranial to the scapula. The skin was lifted using forceps and the tissue was excised using sterile scissors. A circular silicone splint (10 mm diameter) with 0.7 mm diameter opening (Grace Bio Labs, USA) was placed over each wound and anchored in place with 6-0 nylon sutures (Covidien, Canada) to prevent healing by wound contraction [19,20]. Wounds were then left untreated or experimentally infected and treated with the PTT technique as described below. Rats were then monitored in recovery cages under heat lamps and returned to their home cages following recovery of purposeful movement and postural control.

2.8. Safety assessment of PTT technique

Following surgical wound creation (n = 6) as described above, 50 μl of NRs-PVCL solution was applied to the wound. The wound was exposed to diode laser (785 nm) at power density 0.65 W/cm^2 for 40 min, and then covered with a transparent dressing (Tegaderm, JM healthcare, USA). Animals with untreated wounds served as controls. Some animals underwent wound treatment unilaterally, with the contralateral wound serving as control. Animals were euthanized after 72 h, the tissue was excised, fixed in 10% neutral buffered formalin, embedded in paraffin wax, sectioned and stained with hematoxylin and eosin, and examined by a veterinary pathologist without knowledge of wound treatment. Tissues were scored on a scale of 1–4 across 4 parameters for inflammation and 8 for rate of healing.

2.9. Experimental wound infection

Three groups of animals (3 animals/group) were used. The first group comprised animals whose wounds were infected with *E. coli* NEB 10 beta strain (K12 strain) then treated as above using the thermogel and laser application. After laser application, animals were euthanized. The infected tissue was excised, homogenized using tissue homogenizer, serially diluted and plated on ampicillin containing LB agar media for bacteria count. The percentage of living cells was calculated by dividing CFU/ml of treated group by CFU/ml of non-treated group. The second and third groups served as controls. The second group was infected with bacteria and left untreated while the third group's wounds were neither infected nor treated. For the wound healing experiment three groups of animals (3 animals/group) were treated in the same manner as described above but were monitored for wound closure for up to 12 days.

2.10. Statistical analysis

Data were statistically analyzed using SPSS version 20, GraphPad Prism 6 and Microsoft Excel 2013. The student t-test was used for hypothesis testing between data pairs. One-way ANOVA followed by Post HOC Tukey was used for hypothesis testing in data sets with more than two means and one independent variable. Two-way ANOVA was used for hypothesis testing in data sets with more than two means and two independent variable.

3. Results and discussion

3.1. Preparation and characterization of PVCL-NRs nanoformulation

We synthesized NRs using the cetyl trimethylamonnium bromide (CTAB) method pioneered by the El-Sayed and Murphy labs with some slight modifications [17,18]. After synthesis, the surface of CTAB-NRs was modified with m-PEG-SH, which makes the particles more stable in aqueous buffer and reduces their cellular toxicity due to CTAB [21,22]. Figure S1 in the Supporting Information summarizes the characteristics of both CTAB and PEG-NRs. Further, the PEG-NRs were dispersed in a 20% w/v biocompatible [23] thermogel PVCL solution that exhibits a lower critical solution temperature (LCST) of 35 °C (Fig. 1 and Fig. S2 in the Supporting Information). At low temperature, the polymer forms hydrogen bonds with water which leads to polymer dissolution in water. However, when temperature increases to LCST the hydrogen bonds start to break and an increase in the hydrophobic interactions between the polymer moieties become dominant. As a result, the polymer collapse and undergoes phase separation [24]. TEM image demonstrated homogeneous dispersion of NRs inside the PVCL solution (inset in Fig. 1). UV–Vis spectrophotometry confirmed the monodispersity and homogeneity of NRs-PVCL nanosolution (nanosol) by showing two distinct absorbance peaks around 520 nm and 770 nm for the NRs transverse and longitudinal surface plasmon resonance (SPR) (Fig. S2a in the Supporting Information). The data further showed that the presence of NRs in the solution did not affect the transition temperature of the PVCL polymer (Fig. S2c in the Supporting Information). NRs-PVCL nanosol is liquid at temperature below 35 °C (LCST), however, when the solution is exposed to a 785 nm diode laser light, it heats to a temperature higher than 35 °C. As a result, the NRs-PVCL converts into gel state. When the laser is removed, the gel converts back into liquid state (see Fig. 1B).

3.2. Thermal assessment of PVCL as a dispersion medium for GNRs

To test the ability of the NRs-PVCL nanosol to significantly increase the temperature on a surface in comparison to NRs-aqueous solution nanosol, film temperature profiles were developed. The aqueous solution for all experiments was PBS. Experiments were

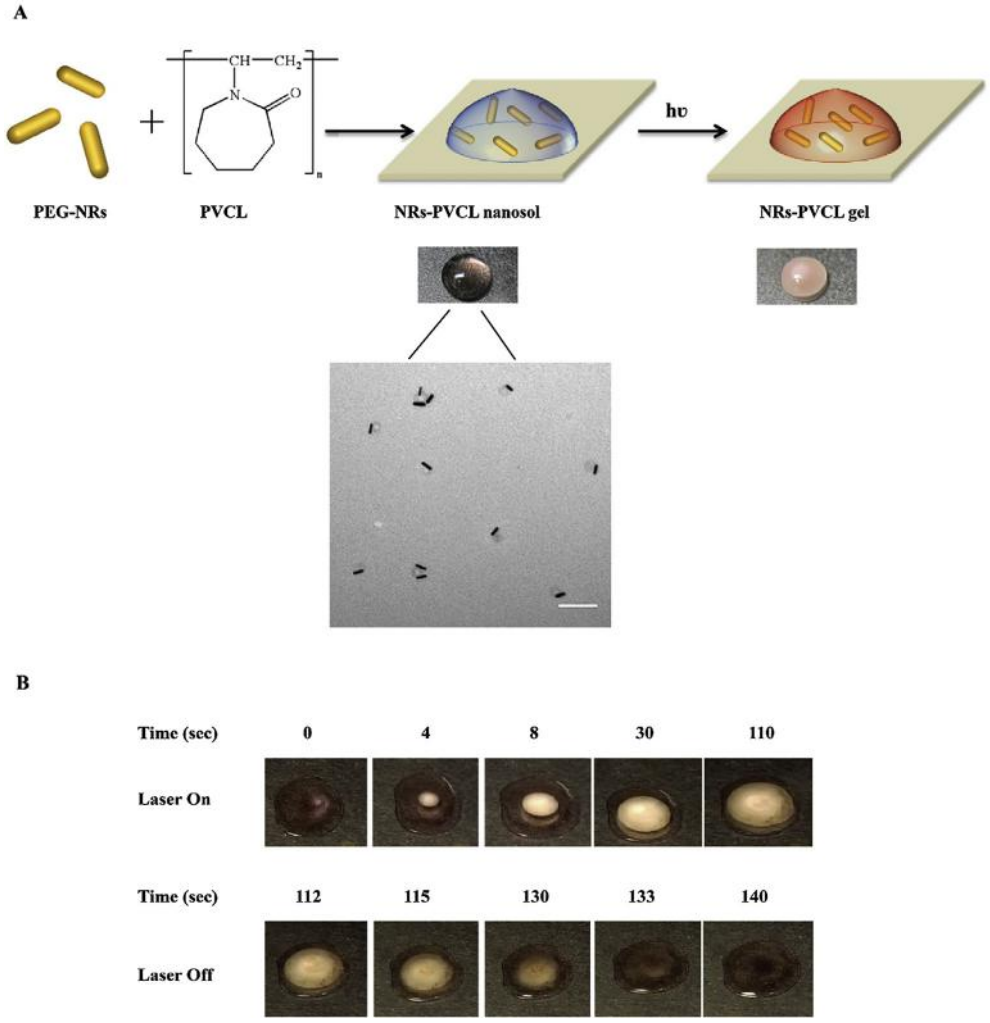

Fig. 1. Characterization of gold nanorods thermogel. (A) Schematic of the liquid nanosol composed of PEG-NRs dispersed in biocompatible PVCL thermogel solution. Inset TEM image represents nanoscale dispersion of NRs embedded in PVCL thin film (scale bar denotes 100 nm). (B) Photos of NRs-PVCL nanosol. The upper panel shows that upon laser exposure, the PVCL exhibits phase transition from sol to gel while the lower panel shows the conversion back to liquid when the laser is turned off.

carried out by placing the nanosols on the surface of a 35 mm Petri dish. The films were then excited with a 785 nm diode laser with an absorbance wavelength that closely matched the absorbance of the longitudinal axis of the NRs for 20 min at 0.65 W/cm^2. For film temperature measurements, a thermal camera was selected because the camera provides a more accurate measurement for surface temperature compared to thermocouples [25]. The emissivity for each individual sample was corrected relative to a reference sample (electrical black tape) with known near perfect emissivity of 0.95. A temperature difference parameter (ΔT_f) was calculated as the difference between the film temperature at time point t ($T_f(t)$) and initial film temperature (T_0) on the surface. After plotting temperature change over time, the data suggested that at the same concentration of NRs and volume of nanosols, both NRs-PBS and NRs-PVCL showed an initial increase in temperature followed by an equilibrium steady-state plateau. The blank solutions of PBS and PVCL (without NRs) did not show any change in temperature under laser excitation (Fig. 2). A significantly higher equilibrium temperature increase of ~12 °C ± 2 °C was detected for NRs-PVCL nanosol ($\Delta T_f \approx 25$ °C ± 2 °C) compared to colloidal NRs-PBS solution ($\Delta T_f \approx 12$ °C ± 2 °C) (Fig. 2). This data suggests that the temperature increase maintained by the NR-PVCL nanosol was 2-fold higher than that obtained for the NRs-PBS nanosol

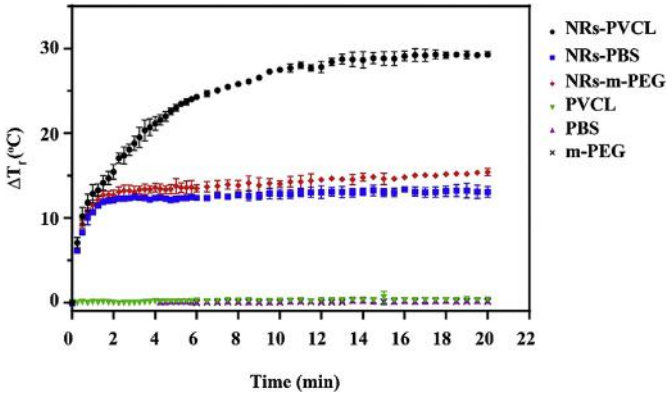

Fig. 2. Temperature profiles. Temperature elevation of NRs-PVCL, NRs-PBS and NRs-PEG solutions (at the same concentration of NRs) exposed to 785 nm CW diode laser (0.65 W/cm^2) as function of exposure time. Blank solution without NRs was used as negative control. Error bars represent standard deviation, where n = 3.

($P < 0.001$). Control samples containing NRs in non-thermogel polymer m-PEG exhibited no polymer transition (Fig. 2) designated as NRs-m-PEG. In addition, the temperature of the film could

be manipulated by altering the laser fluence (W/cm^2), the concentration of NRs, and the irradiation time (Fig. S3 in the Supporting Information). Interestingly, this NRs-PVCL nanosol can be cycled (Fig. S4 in the Supporting Information) on and off, which also suggests that gel can be used multiple times.

We hypothesize that there are two possible mechanisms to explain the difference in temperature of the NRs dispersed in the PVCL and PBS: (1) delayed heat dissipation resulting from sol-to-gel transition; and (2) water evaporation. If one considers the same initial heat generation rates due to the same number of NRs in both media, one can envision that the transition of surrounding medium from a liquid to a gel phase may influence the preservation of heat produced. One possible mechanism that could be responsible for the observed difference in temperature between NRs-PVCL and NRs-PBS nanosols is that the gel slows the dissipation of heat from NRs-PVCL nanosol. Thus, NRs-PVCL can reach higher equilibrium temperature. We examined this by measuring the temperature drop from an equal elevated temperature in both NRs-PVCL and NRs-PBS solutions. To do this, we raised the temperature of both solutions to the same value. We achieved this using different laser fluence for NR-PVCL (0.65 W/cm^2) versus NRs-PBS (1.5 W/cm^2) as our earlier data (Fig. 2) showed that NRs-PVCL exhibited higher temperature than NRs-PBS under same laser fluence. After the temperature of the two solutions reached almost the same point at 10 min of laser exposure, the laser was turned off and the drop in temperature was measured over time. Data in Fig. 3A shows that the heat dissipation rate from NRs-PBS was faster than that from NRs-PVCL with a time constant of 15.15 s versus 33.71 s, respectively ($P < 0.001$). This suggests that the PVCL offers a rigid medium that reduces heat dissipation. A second possible mechanism for the observed temperature difference is water evaporation. To measure the amount of water evaporation, the sample solution was weighed before and after laser exposure and then the amount of water evaporation was measured as a percentage and calculated according to the method described above in Section 2. When NRs-PVCL and NRs-PBS solutions were excited, the NRs generated heat, which caused the evaporation of water from both solutions. However, the amount of water evaporating from the NRs-PBS solution was significantly higher (80%) compared to NRs-PVCL (35%) ($P < 0.001$) (Fig. 3B). This significant water loss can lead to a faster heat dissipation from the solution to the air. As a result, NRs-PBS solution heats to a lower equilibrium temperature. This suggests that both proposed mechanisms could be potentially involved in the temperature differences between the two solutions.

3.3. Assessment of photothermal therapy technique on bacterial survival in-vitro

The thermal properties of the NRs-PVCL nanosol were investigated to determine if they could be applied to kill bacteria. Here, we hypothesize that all bacteria underneath this polymeric blanket would be exposed to the higher temperature generated by the NRs which will enhance the antimicrobial efficacy. Three AMR bacterial strains were investigated: ampicillin-resistant *E. coli*; ampicillin-, gentamicin-, and vancomycin-resistant *A. baumannii*; and vancomycin-resistant *E. faecalis*. These bacterial strains were selected because they are frequently associated with hospital acquired infections of skin and soft tissue, and the urinary and

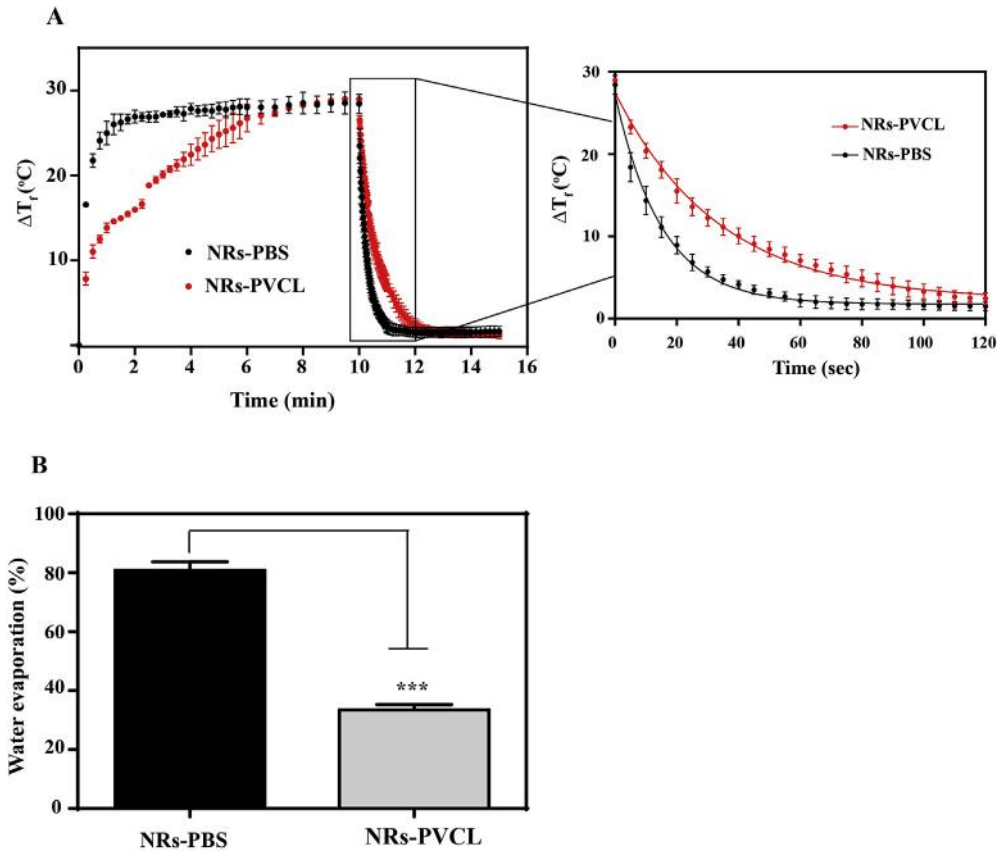

Fig. 3. Heat dissipation and water evaporation from NRs-PVCL and NRs-PBS nanosols. (A) Heat dissipation from NRs-PVCL and NRs-PBS nanosols. Magnified inset represents the heat dissipation rate from the two nanosols as a function of time after laser was turned off. (B) Water evaporation from the two nanosols after 10 min of laser exposure. Error bars represent standard deviation, where n = 3. ***$P < 0.001$.

gastrointestinal tracts [26]. Fig. 4A shows the schematic of our platform. First, all components of the platform were investigated for antimicrobial effect. In the absence of laser application, neither NRs-PBS nor NRs-PVCL nanosols applied on top of contaminated area had antimicrobial effect (Fig. S5a and b in the Supporting Information). This was also confirmed for laser application of blank PBS and blank PVCL solutions (Fig. S5c in the Supporting Information), leaving laser activated heating as the only possible antimicrobial mechanism. Following the control experiments, the effect of laser activated NRs-PVCL on both Gram-positive and Gram-negative antibiotic resistant bacteria was examined under various laser exposure times (10, 20 40 and 60 min) Generally, the increase in exposure time resulted in improved antimicrobial efficacy against both Gram-positive and Gram-negative strains. For the Gram-negative strains (*E. coli* and *A. baumannii*), there was a significant decrease in cell viability of 96% and 94%, respectively, after 40 min of laser exposure ($P < 0.001$) (Fig. 4B and F). Although the Gram-positive strain (*E. faecalis*) was more heat tolerant, the data showed that there is a significant bactericidal effect ($P < 0.001$) of 65% and 50%, respectively, after 40 and 60 min of laser exposure (Fig. 4C). The *E. coli* data suggests that the antimicrobial effect against *E. faecalis* can be enhanced by increasing the temperature via increasing laser power. The antimicrobial efficacy of the NRs-PVCL against *E. coli* was significantly enhanced by about 28% ($P < 0.05$) reaching 99% in 20 min after the laser power was increased from 0.65 to 0.85 W/cm^2 (Fig. 4D). Imaging analysis using TEM showed that the outer membranes of the bacteria were damaged after thermal ablation, leading to loss of structural integrity of bacterial cell walls (Fig. 4G and Fig. S6 in the Supporting Information). It has been shown that heat can melt fatty acids and denature proteins, which in effect results in rupture of cell membranes and subsequent bacterial death [4,27]. To compare to the current plasmonic nanoparticle methods for killing bacteria [28–33], the killing efficiency of our NRs-PVCL was compared to NR-PBS after 20 min of laser exposure at 0.65 W/cm^2 on *E. coli*. Results showed that the NRs-PVCL method achieved 3-fold higher bactericidal activity compared to NR-PBS. The bacterial viability significantly ($P < 0.001$) decreased by ~75% using NRs-PVCL compared to NR-PBS, which did not show antibacterial effect (Fig. 4E).

3.4. Safety assessment of photothermal therapy technique on skin and surrounding tissues

After our technique successfully achieved a significant antimicrobial effect against antimicrobial resistant bacteria in vitro, we were interested to demonstrate the feasibility and applicability of this technique in vivo. We chose an infected excisional wound as an in vivo model to test the ability of our technique to decontaminate infected wounds. First, the safety of the laser-activated NRs-PVCL was evaluated prior to testing its ability to kill bacteria in vivo (see Fig. 5A for experimental design schematic). This was achieved by applying 50 μL of NRs-PVCL solution to an excisional wound created with a standard 5 mm biopsy punch on the dorsum of CD-1 rats. This was followed by laser exposure at 0.65 W/cm^2 for 40 min. Control animals with only wounds were left without any treatment. The animals were euthanized after 72 h and tissue samples were collected and fixed in 10% neutral buffered formalin, embedded in paraffin, sectioned, and stained with hematoxylin and eosin prior to microscopic evaluation. Tissues were scored by a pathologist, Dr. Turner, without knowledge of animal treatment using a scale of 1–4 (0 = normal, 1 = <5% of section affected, 2 = 5–10% of section affected, 3 = >10–30% of section affected, and 4 = >30% of section affected) on 7 inflammation-related parameters (relative numbers of polymorphonuclear leukocytes, macrophages, and lymphocytes, degree of hemorrhage, presence of fibrin, edema, and necrosis) and 2 parameters related to rate of healing (presence of granulation tissue and degree of epithelial regrowth over the wound). There were no significant differences either in inflammation scores or in rate of healing scores between tissues taken from rats that had been subject to laser application as part of the photothermal therapy technique and those that had not undergone laser application (Fig. 5B and Table S1 in the supporting information). Finally, there may be concerns of nanoparticles transporting through the skin. Our previous study shows that the localization of nanoparticles in the skin can be observed by changes in the skin color and the nanoparticles can be imaged using brightfield microscopy after resection and silver staining [34]. After nanorod exposure to the skin, a change in the skin color and the histopathology did not show nanoparticles and thus, we conclude that the nanoparticles were not transported through the skin within the timeframe and concentration used in our study. These results suggest that our treatment method is safe for use on animals.

3.5. Assessment of photothermal therapy technique on bacterial survival in vivo

After establishing the safety of the photothermal technique on the skin and surrounding tissues, the bactericidal effect was investigated using the same excisional wound model. We developed the following methods to show that bacteria can be killed on the skin of a rat. 1–2 × 10^6 CFU of *E. coli* was applied to an excisional wound for 30 min to allow bacteria to attach to the tissue [35]. This was followed by application of 50 μL of NRs-PVCL solution then laser exposure at 0.65 W/cm^2 for 40 min as previously described. Five minutes after treatment, animals were euthanized, wound tissues were excised, homogenized, and serially diluted for bacterial plate count. We selected 5 min because the immune system of the rat can potentially start to attack and kill these surface applied bacteria after 5 min – which would affect our ability to evaluate therapeutic evaluation of the PTT strategy. The results indicated that PTT using NRs-PVCL reduced the bacterial load by 98% ($P < 0.001$) compared to the untreated wounds (Fig. 5C and Fig S7c in the Supporting Information). Moreover, we have demonstrated the effect of our technique on the wound healing process. The technique did not inhibit the wound healing process as the treated wounds healed at the same rate as control wounds (Fig. S7a in the Supporting Information). The infected wounds also healed at the same rate as control wounds. This could be due to the non-invasiveness of this strain of *E. coli,* which can be cleared by the immune system [35]. During the course of wound healing no weight loss was observed (Fig. S7b in the Supporting Information), further demonstrating the safety of the technique. Further studies are needed to determine if AMR bacteria such as methicillin-resistant *Staphylococcus aureus* would be similarly susceptible to the bactericidal effects of the photothermal therapy technique described here. However, such studies would require specialized biosafety facilities but these studies are required to establish the therapeutic effectiveness of the gold nanorod-thermogel treatment system.

4. Conclusion

In conclusion, our study demonstrated that a combination of a thermosensitive biocompatible polymer and gold nanoparticles can significantly reduce the bacterial load in vitro and in vivo. First, we demonstrated that our PTT technique successfully reduced the bacterial load in vitro by 94–96% for Gram negative bacteria and by 65% for Gram positive bacteria. This technique also, reduced the bacterial load in experimentally infected wounds by 98%. Although

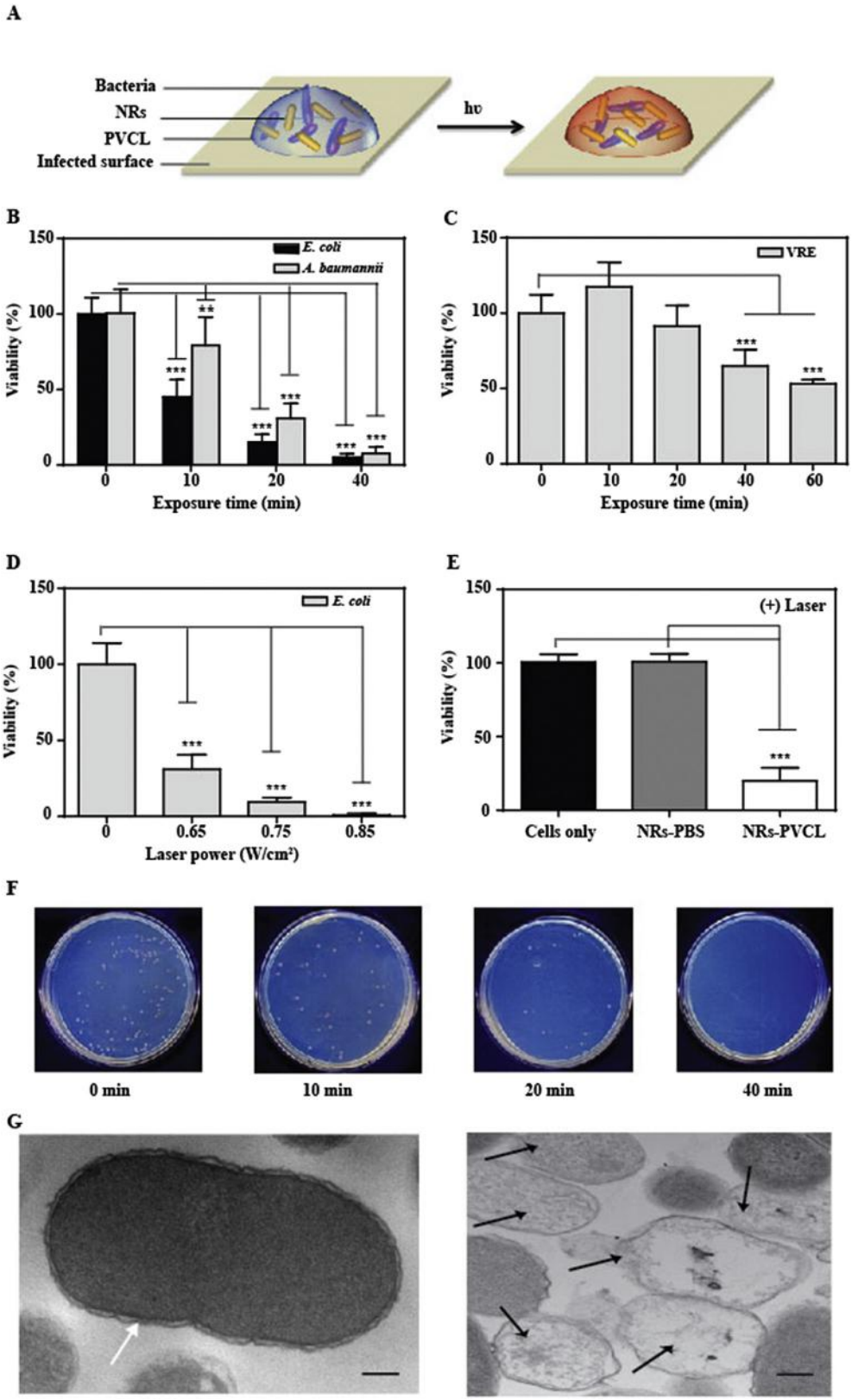

Fig. 4. Photothermal effect of gold nanorods thermogel nanosol on gram (−ve) and gram (+ve) bacteria. (A) Schematic representation of the antibacterial effect of NRs-PVCL (B) Anti-bacterial effect on gram (−ve) strains *E. coli* and *A. baumannii* and (C) on gram (+ve) strain *E. faecalis* after incubation with NRs-PVCL followed by laser irradiation (0.65 W/cm^2) for 10, 20, 40 and 60 min. Generally, there was a significant antibacterial effect on the two types of bacteria as a function of exposure time however, the antibacterial effect was more pronounced on gram (−ve) strains compared to the gram (+ve) strain. (D) The enhancement of the anti bacterial effect of PVCL-NRs on *E. coli* by increasing laser power. (E) Comparison between antibacterial effect of NRs-PVCL and NRs-PBS after 20 min of laser exposure on *E. coli*. Only NRs-PVCL had significant antibacterial affect compared to NRs-PBS solution. (F) Photos of *E. coli* colonies on Luria agar plates show the decrease in the colonies number as a function of exposure time to NRs-PVCL + Laser. (G) TEM image of *E. coli* cells that were exposed to NIR laser (0.65 W/cm^2) for 20 min. The image to the left shows the cells without treatment while the image to the right shows the cells after treatment. White Arrows indicate the areas of cell membrane while the black arrow indicates cell membrane disruption (scale bars denote 160 nm). Error bars represent standard deviation, where n > 3. $^{**}P < 0.01$, $^{***}P < 0.001$. VRE refers to the bacteria *E. faecalis*.

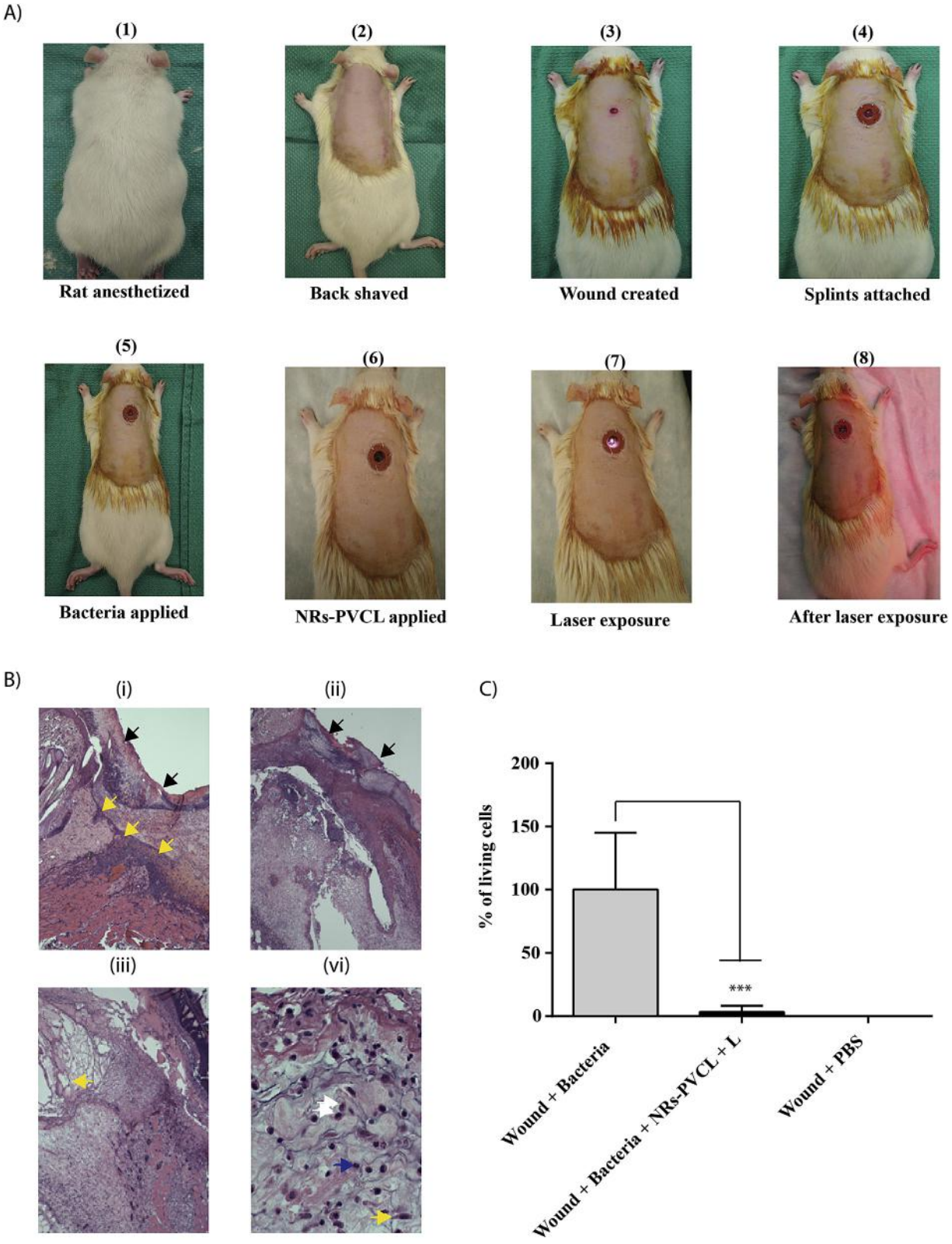

Fig. 5. In-vivo experiments to evaluate the PTT technique. (A) Schematic representation of the experimental design. (B) Photomicrographs of the safety assessment of the PTT technique. Wounds treated with thermogel and laser (0.65 W/cm^2 for 40 min) or control wounds without treatment. There were no remarkable differences in either inflammation or healing rates between treatment groups. i) Control wound (×200) with serocellular crust (black arrows), moderate to marked mixed leukocytic infiltrate and re-epithelialization (yellow arrows) ii) Wound treated with thermogel and laser (×200) with serocellular crust (black arrows), moderate to marked mixed leukocytic infiltrate and loose granulation tissue in the mid to lower left of the image. iii) Control wound (×400) with granulation tissue subtending the wound bed with strands of fibrin (fine, thread-like pink strands, yellow arrow). iv) Wound treated with thermogel and laser (×400) with inflammatory cell infiltrate (macrophages, white arrows; and neutrophil, blue arrow), and evidence of early granulation (fibroblast, yellow arrow). (C) Antimicrobial effect of NR-PVCL and laser in infected wounds after 40 min of laser exposure at laser fluence of 0.65 W/cm^2. There was a significant reduction in bacterial load in the treated vs untreated wounds. Error bars represent standard deviation, where n = 3. ***P < 0.001. (For interpretation of the references to color in this figure legend, the reader is referred to the web version of this article.)

the *E. coli* strain used in the in vivo study was not pathogenic, we hypothesize that this technique would be equally effective against AMR bacteria based on the in vitro results. Further testing is required to confirm this hypothesis. Interestingly, *A. baumannii* is considered an emerging cause of health care-associated infections, including those of skin and soft tissue [36,37]. Additional investigation is required to establish the efficacy of the PTT technique described on more common causes of skin and soft tissue infections, such as methicillin-resistant *S. aureus*.

Unlike antimicrobials or other chemotherapeutics (e.g. silver-based materials, mafenide acetate, mupirocin, and polysoporin (polymyxin *B*) in which the mechanism of bacterial killing is based on the binding of the drug to a specific target within or on the bacterial cell wall, the PTT technique does not depend on bacterial binding. Antimicrobial chemotherapeutics are also limited in the spectrum of bacteria against which they are effective, being classified as effective against Gram-negative or Gram-positive bacteria or both. Additionally, these agents have potentially serious risks following prolonged or incorrect use, such as cytotoxicity accompanied by a delay in wound healing and risk of antimicrobial resistance [38–47]. In contrast, the PTT technique demonstrates bactericidal activity against both Gram-positive and Gram-negative bacteria by means of physical destruction of bacterial cell components. This mechanism of action circumvents standard modes of AMR and may be applied without requirement for preliminary culture and sensitivity testing, speeding the onset of therapy. In addition, this technique has the following characteristics: i) is simple to prepare and apply; ii) does not affect the stability of the dispersed NPs; iii) can be excited by low laser power that can be provided by a hand held laser device; and iv) is safe and has minimal effect on surrounding tissue or the healing process.

Acknowledgment

WCWC acknowledges the Canadian Institutes of Health Research (MOP-93532; G118160781), Natural Sciences and Engineering Research Council of Canada (NETGP 35015-07, RGPIN 288231-09 and 203312-08), Canadian Research Chairs Program (950-203403), Canadian Foundation for Innovation, and Ontario Ministry of Research and Innovation for funding support. MAAM acknowledges the ministry of higher education (mission sector) in Egypt and Egyptian cultural & educational bureau in Canada for funding and Mr. Leo Chou for helping in bacterial TEM imaging. Also, WCWC and MAAM acknowledge Mr. Rainer Deguzman for performing all the animal surgery, Mr. Stephen Perusini for his discussions, Prof. John Bischof, Mr. Qin Dai, Mr. Yih Yang Chen for reading the manuscript, and Prof. Justin Nodwell for providing space in his lab for doing the bacterial experiments.

Appendix A. Supplementary data

Supplementary data related to this article can be found at http://dx.doi.org/10.1016/j.biomaterials.2016.04.009.

References

[1] Prevention Center for Disease Control and, Antibiotic Resistance Threats in the United States, 2013.
[2] J.A. Suaya, R.M. Mera, A. Cassidy, P.O. Hara, H. Amrine-madsen, S. Burstin, et al., Incidence and cost of hospitalizations associated with *Staphylococcus aureus* skin and soft tissue infections in the United States from 2001 through 2009, BMC Infect. Dis. 14 (2014) 1–8.
[3] J.A. Suaya, D.F. Eisenberg, C. Fang, L.G. Miller, Skin and soft tissue infections and associated complications among commercially insured patients aged 0 – 64 years with and without diabetes in the U.S, PLoS One 8 (2013) 1–8.
[4] A. Mrozik, S. Łabużek, Cytoplasmatic bacterial membrane responses to environmental perturbations, Polish J. Environ. Stud. 13 (2004) 487–494.
[5] R.W.Y. Habash, R. Bansal, D. Krewski, H.T. Alhafid, Thermal therapy, part 2: hyperthermia techniques, Crit. Rev. Biomed. Eng. 34 (2006) 491–542.
[6] Z. Qin, W.C.W. Chan, D.R. Boulware, T. Akkin, E.K. Butler, J.C. Bischof, Significantly improved analytical sensitivity of lateral flow immunoassays by using thermal contrast, Angew. Chem. Int. Ed. Engl. 51 (2012) 4358–4361.
[7] M. Wu, A.R. Deokar, J. Liao, P. Shih, Y. Ling, Graphene-based photothermal agent for rapid and effective killing of bacteria, ACS Nano 7 (2013) 1281–1290.
[8] J.T. Robinson, S.M. Tabakman, Y. Liang, H. Wang, H.S. Casalongue, D. Vinh, et al., Ultrasmall reduced graphene oxide with high near-infrared absorbance for photothermal therapy, J. Am. Chem. Soc. 133 (2011) 6825–6831.
[9] K. Pu, A.J. Shuhendler, J.V. Jokerst, J. Mei, S.S. Gambhir, Z. Bao, et al., Semiconducting polymer nanoparticles as photoacoustic molecular imaging probes in living mice, Nat. Nanotechnol. 9 (2014) 233–239.
[10] Z. Qin, J.C. Bischof, Thermophysical and biological responses of gold nanoparticle laser heating, Chem. Soc. Rev. 41 (2012) 1191–1217.
[11] Liangran Gou, D.D. Yan, D. Yang, L. Yajuan, X. Wang, Z. Olivia, et al., Combinatorial photothermal and immuno Cancer therapy using chitosan-coated hollow copper sulfide nanoparticles, ACS Nano 8 (2014) 5670–5681.
[12] J. Yang, D. Shen, L. Zhou, W. Li, X. Li, C. Yao, et al., Spatially confined fabrication of core-shell gold nanocages@Mesoporous silica for near-infrared controlled photothermal drug release, Chem. Mater. 25 (2013) 3030–3037.
[13] A.F. Bagley, S. Hill, G.S. Rogers, S.N. Bhatia, Plasmonic photothermal heating of intraperitoneal tumors through the use of an implanted near-infrared source, ACS Nano 7 (2013) 8089–8097.
[14] E.B. Dickerson, E.C. Dreaden, X. Huang, I.H. El-Sayed, H. Chu, S. Pushpanketh, et al., Gold nanorod assisted near-infrared plasmonic photothermal therapy (PPTT) of squamous cell carcinoma in mice, Cancer Lett. 269 (2008) 57–66.
[15] F.-Y. Cheng, C.-T. Chen, C.-S. Yeh, Comparative efficiencies of photothermal destruction of malignant cells using antibody-coated silica@Au nanoshells, hollow Au/Ag nanospheres and Au nanorods, Nanotechnology 20 (2009) 425104.
[16] J.-O. You, P. Guo, D.T. Auguste, A drug-delivery vehicle combining the targeting and thermal ablation of HER2+ breast-cancer cells with triggered drug release, Angew. Chem. Int. Ed. Engl. 52 (2013) 4141–4146.
[17] B. Nikoobakht, M.A. El-sayed, Preparation and growth mechanism of gold nanorods (NRs) using seed-mediated growth method, Chem. Mater. (2003) 1957–1962.
[18] A. Gole, C.J. Murphy, Seed-mediated synthesis of gold nanorods: role of the size and nature of the seed, Chem. Mater. 16 (2004) 3633–3640.
[19] L. Dunn, H.C.G. Prosser, J.T.M. Tan, L.Z. Vanags, M.K.C. Ng, C.A. Bursill, Murine model of wound healing, J. Vis. Exp. (2013) e50265.
[20] X. Wang, J. Ge, E.E. Tredget, Y. Wu, The mouse excisional wound splinting model, including applications for stem cell transplantation, Nat. Protoc. 8 (2013) 302–309.
[21] A.M. Alkilany, P.K. Nagaria, C.R. Hexel, T.J. Shaw, C.J. Murphy, M.D. Wyatt, Cellular uptake and cytotoxicity of gold nanorods: molecular origin of cytotoxicity and surface effects, Small 5 (2009) 701–708.
[22] C. Grabinski, N. Schaeublin, A. Wijaya, H. D'Couto, S.H. Baxamusa, K. Hamad-Schifferli, et al., Effect of gold nanorod surface chemistry on cellular response, ACS Nano 5 (2011) 2870–2879.
[23] H. Vihola, A. Laukkanen, L. Valtola, H. Tenhu, J. Hirvonen, Cytotoxicity of thermosensitive polymers poly(N-isopropylacrylamide), poly(N-vinylcaprolactam) and amphiphilically modified poly(N-vinylcaprolactam), Biomaterials 26 (2005) 3055–3064.
[24] Y. Qiu, K. Park, Environment-sensitive hydrogels for drug delivery, Adv. Drug Deliv. Rev. 64 (2012) 49–60.
[25] R.D. Lucier, I guess if I really wanted to measure surface temperature, I would just use a thermocouple: understanding the challenges of surface temperature measurements, InfraMation 2011 Proc. (2011) 1–12.
[26] World Health Organization, Prevention of Hospital-acquired Infections, World Health Organization, 2002. WHO/CDC/EPH/2002.12.
[27] N. Katsui, T. Tsuchido, R. Hiramatsu, S. Fujikawa, M. Takano, I. Shibasaki, Heat-induced blebbing and vesiculation of the outer membrane of *Escherichia coli*, J. Bacteriol. 151 (1982) 1523–1531.
[28] R.S. Norman, J.W. Stone, A. Gole, C.J. Murphy, T.L. Sabo-attwood, Targeted photothermal lysis of the pathogenic bacteria, *Pseudomonas aeruginosa*, with gold nanorods, Nano Lett. 8 (2008) 302–306.
[29] W.-S. Kuo, C.-N. Chang, Y.-T. Chang, C.-S. Yeh, Antimicrobial gold nanorods with dual-modality photodynamic inactivation and hyperthermia, Chem. Commun. (Camb) (2009) 4853–4855.
[30] S.A. Khan, A.K. Singh, D. Senapati, Z. Fan, P.C. Ray, Bio-conjugated popcorn shaped gold nanoparticles for targeted photothermal killing of multiple drug resistant Salmonella DT104, J. Mater. Chem. 21 (2011) 17705.
[31] Y. Zhu, M. Ramasamy, D.K. Yi, Antibacterial activity of ordered gold nanorod arrays, ACS Appl. Mater. Interfaces 6 (2014) 15078–15085.
[32] J.C. Castillo-martínez, G.A. Martínez-castañón, F. Martínez-gutierrez, N.V. Zavala-alonso, N. Patiño-marín, N. Niño-martinez, Antibacterial and antibiofilm activities of the photothermal therapy using gold nanorods against seven different bacterial strains, J. Nanomater. 2015 (2015) 1–7.
[33] C.-B. Kim, D.K. Yi, P.S.S. Kim, W. Lee, M.J. Kim, Rapid photothermal lysis of the pathogenic bacteria, *Escherichia coli* using synthesis of gold nanorods, J. Nanosci. Nanotechnol. 9 (2009) 2841–2845.
[34] E. Sykes, Q. Dai, K.M. Tsoi, D.M. Hwang, W.C.W. Chan, Nanoparticle exposure in animals can be visualized in the skin and analysed via skin biopsy, Nat.

Comm. 5 (2013) 3796.
[35] M.R. Hamblin, D.A. O'Donnell, N. Murthy, C.H. Contag, T. Hasan, Rapid control of wound infections by targeted photodynamic therapy monitored by in vivo bioluminescence imaging, Photochem. Photobiol. 75 (2002) 51–57.
[36] A. Michalopoulos, M.E. Falagas, A. Michalopoulos, M.E. Falagas, Treatment of acinetobacter infections treatment of acinetobacter infections, Expert Opin. Pharmacother. 11 (2010) 779–788.
[37] F. Perez, N.G. Conger, J.S. Solomkin, Acinetobacteria baumannii-associated skin and soft tissue infections: recognizing a broadening spectrum of disease, Surg. Infect. (Larchmt) 11 (2010) 49–57.
[38] W.W. Monafo, B. Freedman, Topical therapy for burns, Surg. Clin. North Am. 67 (1987) 133–145.
[39] I.A. Holder, S.T. Boyce, Assessment of the potential for microbial resistance to topical use of multiple antimicrobial agents, Wound Repair Regen. 7 (1999) 238–243.
[40] C.J. Coombs, A.T. Wan, J.P. Masterton, R.A. Conyers, J. Pedersen, Y.T. Chia, Do burn patients have a silver lining? Burns 18 (1992) 179–184.
[41] I.O. Leitch, A. Kucukcelebi, M.C. Robson, Inhibition of wound contraction by topical antimicrobials, Aust. N. Z. J. Surg. 63 (1993) 289–293.
[42] G.L. McHugh, R.C. Moellering, C.C. Hopkins, M.N. Swartz, Salmonella typhimurium resistant to silver nitrate, chloramphenicol, and ampicillin, Lancet 1 (1975) 235–240.
[43] K. Bridges, A. Kidson, E.J. Lowbury, M.D. Wilkins, Gentamicin- and silver-resistant pseudomonas in a burns unit, Br. Med. J. 1 (1979) 446–449.
[44] A.T. Hendry, I.O. Stewart, Silver-resistant Enterobacteriaceae from hospital patients, Can. J. Microbiol. 25 (1979) 915–921.
[45] R. Herruzo-Cabrera, V. Garcia-Torres, J. Rey-Calero, M.J. Vizcaino-Alcaide, Evaluation of the penetration strength, bactericidal efficacy and spectrum of action of several antimicrobial creams against isolated microorganisms in a burn centre, Burns 18 (1992) 39–44.
[46] J.B. Patel, R.J. Gorwitz, J.A. Jernigan, Mupirocin resistance, Clin. Infect. Dis. 49 (2009) 935–941.
[47] A.E. Simor, T.L. Stuart, L. Louie, C. Watt, M. Ofner-Agostini, D. Gravel, et al., Mupirocin-resistant, methicillin-resistant *Staphylococcus aureus* strains in Canadian hospitals, Antimicrob. Agents Chemother. 51 (2007) 3880–3886.